Available online at www.sciencedirect.com

SciVerse ScienceDirect

Ceramics International 39 (2013) 469–474

CERAMICS INTERNATIONAL

www.elsevier.com/locate/ceramint

# Structural and optical studies on sol–gel derived ZnO thin films by excimer laser annealing

Chien-Yie Tsay*, Min-Chi Wang

*Department of Materials Science and Engineering, Feng Chia University, Taichung 40724, Taiwan*

Received 25 April 2012; received in revised form 17 June 2012; accepted 17 June 2012
Available online 23 June 2012

**Abstract**

High-quality polycrystalline ZnO thin films were deposited onto alkali-free glasses at a temperature of 300°C in air ambience by combining sol–gel spin coating and KrF excimer laser annealing. The effects of laser irradiation energy density on the crystallization, microstructure, surface morphology, and optical transmittance of as-prepared ZnO thin films were investigated and compared to the results of thermally annealed ZnO thin films. The crystallinity level and average crystallite size of laser annealed ZnO thin films increased as laser energy density increased. The crystallinity levels and average crystallite size of excimer laser annealed (ELA) thin films were greater than those of the thermally annealed (TA) thin films. However, laser annealed thin films had abnormal grain growth when irradiation energy density was 175 mJ/cm$^2$. Experimental results indicated that the optimum irradiation energy density for excimer laser annealing of ZnO sol–gel films was 150 mJ/cm$^2$. The ELA 150 thin films had a dense microstructure, an RMS roughness value of 5.30 nm, and an optical band gap of 3.38 eV, close to the band gap of a ZnO crystal (3.4 eV).


*Keywords:* A. Films; A. Sol–gel processes; B. Microstructure-final; D. ZnO

## 1. Introduction

Zinc oxide (ZnO) is a II–VI group, n-type conductivity, and direct wide band gap semiconductor. Polycrystalline ZnO thin films have attracted interest for application in various optoelectronic devices [1–5], chemical sensors [6], and biosensors [7] because of their low cost, ease of manufacture, and specific electrical and optical properties. For example, impurity-doped ZnO conductive films could be used for replacing conventional transparent conducting oxide (TCO) films of indium tin oxide (ITO) as the transparent electrode in liquid crystal display panels [8]. In the past few years, ZnO-based semiconductor thin films have been developed as a replacement for hydrogenated amorphous silicon (*a*-Si:H) thin films as the active layer in thin film transistors (TFTs) [1,2,9]. In addition, they also are emerging as a prospective alternative to gallium nitride (GaN) as the absorption layer in ultraviolet (UV) detectors [3].

Fabricating functional metal oxide films by solution-based processes, such as the sol–gel process, is simpler, has higher throughput, allows easier composition modification, and costs less than vacuum deposition methods such as RF sputtering or pulsed laser deposition (PLD). The sol–gel process can be combined with the micro- or nano-scale printing techniques such as inkjet printing and microcontact printing to allow direct patterning of conducting oxide electrodes and oxide semiconductor layers for active optoelectronic devices. Most solution-processed metal oxide films require thermal annealing at a high temperature ($\geq$400 °C) for decomposition, oxidation, and densification of as-coated precursor films [1,10]. However, high temperature annealing processes will degenerate the contact resistance between the metal electrode and semiconductor layer, leading to undesirable side effects during device fabrication [11]. In addition, solution-based processes also produce films of lower quality and finer grain size than those of the sputtered films. These features will degrade the electrical and optical properties of the films and limit their applications.

The electrical and optical properties of ZnO thin films are greatly affected by their chemical composition and

*Corresponding author. Tel.: +886 4 24517250; fax: +886 4 24510014.
*E-mail address:* cytsay@fcu.edu.tw (C.-Y. Tsay).

0272-8842/$36.00 
http://dx.doi.org/10.1016/j.ceramint.2012.06.050

crystallographic characteristics [12]. Bao et al. reported that in ZnO thin films, high crystallinity contributed to low electrical resistivity [13]. Such films may also have a high carrier concentration and fast carrier mobility. Hence, deposition methods and fabrication processes for obtaining high quality ZnO thin films need to be developed. One possibility is the excimer laser annealing (ELA) process, which has been utilized to improve the electrical properties of oxide semiconductor films [14–16]. Excimer laser irradiation can be used to selectively raise the temperature for a very short time (some tens of nanoseconds) at a specific position on an oxide semiconductor film without causing heat damage to the underlayer or substrate [15]. That is, the excimer laser irradiation can be used in a low-thermal-budget annealing process [16].

Many studies have discussed the physical properties of sputtered or pulsed laser deposited ZnO-based thin films annealed by excimer laser. However, only a few research groups have reported on excimer laser annealing on sol–gel derived crystalline ZnO-based thin films. Nagase et al. prepared crystalline ZnO thin films on quartz glass substrates by KrF excimer laser irradiation of sol–gel derived precursors [12,17]. Dried ZnO sol–gel films annealed at threshold energy fluence exhibited green photoluminescence (PL) and had closed-packed columnar crystal in the upper layer. Tsang et al. fabricated transparent conducting Al-doped ZnO (AZO) thin films by KrF excimer laser irradiation of sol–gel spin-coated films [18]. They reported that the electrical and optical characteristics of sol–gel derived AZO thin films were significantly improved by excimer laser irradiation. Recently, Kim et al. deposited ZnO thin films on sapphire substrates by sol–gel process before excimer laser annealing [19]. The excimer laser annealed ZnO thin films showed intense near-band-edge (NBE) emission and weak deep-level emission.

In this study, high quality ZnO thin films were prepared by sol–gel spin coating followed by KrF excimer laser annealing. The influences of various energy densities of laser irradiation on the crystallinity, structures, surface morphologies, and optical properties of the ZnO thin films were investigated. In addition, the properties of ZnO thin films prepared by thermal annealing and excimer laser annealing were compared.

## 2. Experimental

A precursor solution was synthesized by dissolving zinc acetate dihydrate in 2-methoxyethano (2-ME), and then a stabilizer of monoethanolamine (MEA) was added to the blended solution. The concentration of zinc ions was 0.75 M, and the molar ratio of MEA to zinc ions was maintained at 1.0. The solution was stirred at 60 °C for 2 h to yield a clear and transparent sol. All ZnO sol–gel films were spin coated onto pre-cleaned NEG OA-10 glass substrates with a size of 50 mm × 50 mm and a thickness of 0.7 mm at a rotation speed of 3000 rpm for 30 s. Each as-coated film was heated from room temperature to 300 °C at a heating rate of 4 °C/min and then maintained at 300 °C for 10 min to evaporate the solvent, water, and organics. After the spin coating and drying procedures were repeated three times, these dried sol–gel films were given heat treatment with KrF excimer laser annealing (ELA) or conventional thermal annealing (TA) to achieve crystalline ZnO thin films.

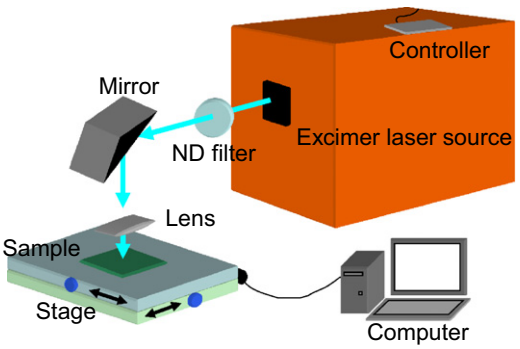


Fig. 1. Schematic of the experimental setup used for excimer laser annealing of ZnO sol–gel films.

The dried sol–gel films were irradiated by KrF excimer laser (wavelength 248 nm) using a Lambda Physic type COMPex 301F laser source. The setup of excimer laser irradiation used for annealing the dried ZnO sol–gel films is illustrated in Fig. 1. The number of impinging shots was maintained at 15, and the frequency of the laser shot was fixed at 7 Hz. The laser beam had a size of 2.5 cm × 0.15 cm, and the energy density of laser irradiation ranged from 100 to 175 mJ/cm$^2$ (in steps of 25 mJ/cm$^2$). For thermally-annealed samples, portions of dried sol–gel films were heat treated at 500 °C for 1 h in a tube furnace under air ambiance.

The crystallinity levels of dried ZnO sol–gel films and the two kinds of annealed ZnO thin films were examined by X-ray diffractometer (XRD, MAC Science MXP3) with Cu-K$\alpha$ radiation ($\lambda$=1.5406 Å). Plane-view micrographs of annealed ZnO thin films were taken with a field-emission scanning electron microscope (FE-SEM, Hitachi S-4800) for examination of the structural changes. The surface morphology and root mean square (RMS) roughness level of the films were examined by tapping mode scanning probe microscopy (SPM, Digital Instrument NS4/D3100CL/MultiMode). Optical transmittance spectra of these films were measured with a UV–vis spectrophotometer (Mini-D2T, Ocean Optics Inc.).

## 3. Results and discussion

X-ray diffraction patterns of the dried sol–gel film, thermally annealed thin film, and dried sol–gel films annealed with different laser energy densities are shown in Fig. 2. According to our previous report, most organic compounds in the ZnO sol–gel films evaporate and/or decompose after heating to 300 °C [20]. Thus the as-coated sol–gel films were dried at 300 °C. Moreover, Tsang et al. have reported that 300 °C is a suitable temperature to induce crystal growth in the AZO sol–gel films, for the drying

treatment obviously enhanced the 248 nm excimer laser absorption of the dried AZO sol–gel films [18]. The XRD pattern of dried sol–gel film has weak diffraction signals on the (100), (002), (101), (110), and (112) planes (spectrum of (i) in Fig. 2). These signals indicated that the film had a crystalline phase but a low crystallinity level.

XRD patterns reveal these annealed ZnO thin films were polycrystalline with a hexagonal wurtzite structure. The diffraction patterns corresponded to seven diffraction peaks of the standard JCPDS 36-1451 of the ZnO crystal. The XRD patterns of excimer laser annealed (ELA) thin films display sharp diffraction peaks, and the full widths at half-maximum (FWHMs) for three main diffraction peaks, (100), (002), and (101), are narrower than those of the thermally annealed (TA) thin film.

The crystallite sizes of polycrystalline thin films can be estimated using the Scherrer formula. Fig. 4 shows that the calculated average crystallite sizes for the three main diffraction peaks of the (100), (002), and (101) planes varied with laser energy density. The average crystallite size of the ELA 100 thin film was 14.76 nm. When the laser energy density was increased from 125 to 175 mJ/cm$^2$, the average crystallite size increased from 17.90 to 20.17 nm. It is worthy to note that the TA thin film's average crystallite size was 9.30 nm (Table 1), which was only about one-half that of the thin films annealed with a higher laser energy density (ELA 150 and ELA 175). Those results suggested that grain growth of the ZnO films was significantly greater with excimer laser annealing than with thermal annealing, and that grain growth was faster when laser energy density was higher.

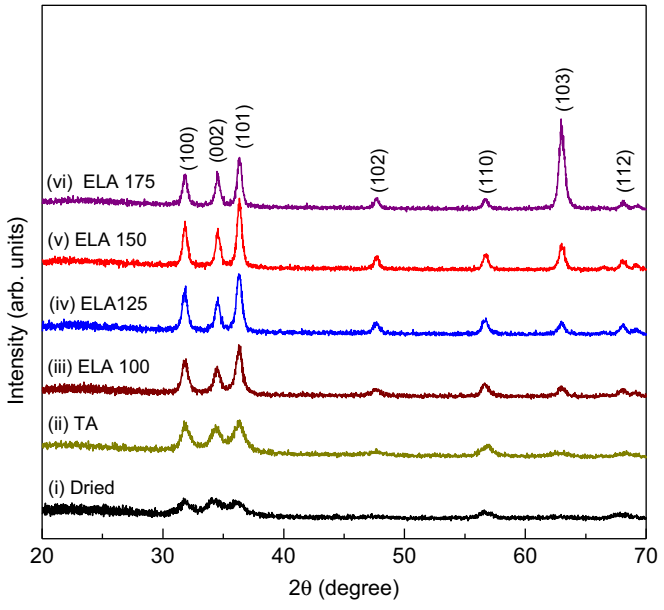


Fig. 2. X-ray diffraction patterns of the dried sol–gel film, thermally annealed (TA) and excimer laser annealed (ELA) ZnO thin films.

The $a$- and $c$-lattice parameters of TA and ELA 150 thin films were calculated from the (100) and (002) peaks using the formulas $a=\lambda/\sqrt{3}\sin\theta$ and $c=\lambda/\sin\theta$, respectively. The $a$- and $c$-lattice parameters of the TA thin film were 3.251 Å and 5.216 Å, which are very close to the parameters of hexagonal ZnO crystal ($a=3.250$ Å and $c=5.207$ Å) [21]. It was found that the lattice parameters of the ELA 150 thin film, $a=3.243$ Å and $c=5.186$ Å, were smaller than that of the TA thin film. Nagase et al. reported that the excimer laser annealing process could produce larger oxygen vacancies more efficiently than the thermal annealing process [12]. Thus, the lower lattice parameter values can be attributed to the resultant oxygen vacancies. They also proposed that the thermally annealed films exhibited high sheet resistance mainly due to a lack of oxygen vacancies. Thus, the decrease in the sheet resistance of excimer laser annealed films can be explained by the presence of oxygen vacancies, which produced conduction electrons.

In addition, the diffraction peaks of high index planes, such as (102), (103), and (112), for ELA thin films are significant. The above discussion has clearly demonstrated that the excimer laser annealing process can significantly raise the crystallinity level and grain size higher than those found in sol–gel derived ZnO thin films prepared by thermal annealing. According to the standard card (JCPDS 36-1451), the XRD pattern of ZnO crystal exhibits the strongest intensity in the (101) diffraction peak, and the relative intensity of $(I_{(101)}/I_{(100)+(002)+(101)})$ is 0.497. In the present study, the diffraction intensities of the three main diffraction peaks for the TA thin film were close (spectrum of (ii) in Fig. 2), and the relative intensity of $(I_{(101)}/I_{(100)+(002)+(101)})$ was 0.363 (Table 1). That feature indicates that the growth rates on the (100), (002), and (101) planes of the TA thin film were very close. Fig. 2 also shows that three ELA thin films (spectra of (iii)–(v)) exhibited strong growth orientation along the (101) plane, similar to typical hexagonal ZnO crystal. Moreover, the

Table 1
Comparison of the structures, surface RMS roughness, and optical properties of thermally annealed and 150 mJ/cm$^2$ excimer laser annealed ZnO thin films.

| Annealing treatment | Relative intensity of $(I_{(101)}/I_{(100)+(002)+(101)})$ | Average crystallite size (nm) | RMS roughness (nm) | Transmittance range[a] (%) | Optical band gap (eV) |
|---|---|---|---|---|---|
| TA | 0.363 | 9.30 | 7.60 | 67.6–87.0 | 3.24 |
| ELA 150 | 0.454 | 19.94 | 5.30 | 72.4–83.0 | 3.38 |

TA: thermally annealed samples; ELA 150: excimer laser annealed samples at an energy density of 150 mJ/cm$^2$.
[a]The values of transmittance range are presented as the data of wavelengths between 400 and 800 nm.

value of the relative intensity of $(I_{(101)}/I_{(100)+(002)+(101)})$ for ELA thin films increased with laser energy densities up to 150 mJ/cm$^2$ (0.454) (Table 1). That is, the excimer laser annealing encouraged grain growth along the (101) plane in the present study. It is also noted that the XRD pattern of the ELA 175 thin film had the strongest intensity at the diffraction peak of (103) (spectrum of (vi) in Fig. 2). That signal reveals that the film had abnormal grain growth along the (103) plane.

The SPM image of the surface of the TA thin film is shown in Fig. 3 (a). The RMS roughness was 7.60 nm. SPM images of the surface of the ELA ZnO thin films exhibited two kinds of surface morphology. Dried sol–gel films annealed with lower energy densities (100 and 125 mJ/cm$^2$) had irregular and rugged surfaces (Fig. 3(b)), while dried sol–gel films annealed with higher energy densities (150 and 175 mJ/cm$^2$) had dense and granular-like surfaces (Fig. 3(c)). The variation of surface root-mean-square (RMS) levels of ELA thin films with laser energy density can be seen in Fig. 4. That plot shows that the value of RMS roughness decreased as laser energy density was increased to 150 mJ/cm$^2$, but it slightly increased when energy density rose higher than that. RMS roughness level improved

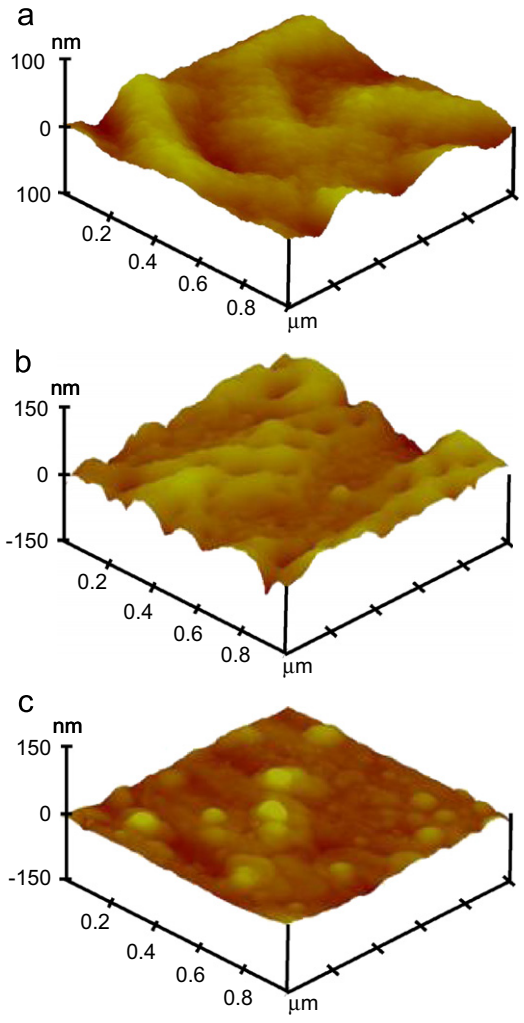


Fig. 3. SPM images of surface of (a) thermally annealed (TA) thin film and dried sol–gel films annealed at energy densities of (b) 100 mJ/cm$^2$ (ELA 100), and (c) 150 mJ/cm$^2$ (ELA 150).

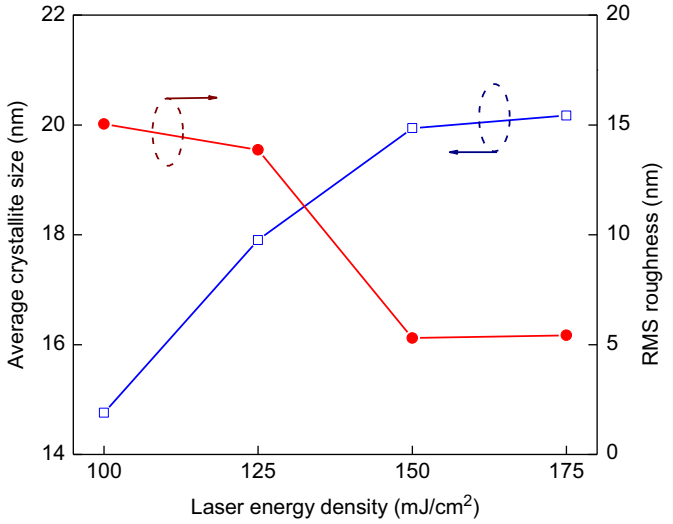


Fig. 4. Variation of average crystallite size and RMS roughness value of excimer laser annealed (ELA) ZnO thin films with laser energy density.

significantly when laser energy density was increased from 125 to 150 mJ/cm$^2$.

It is well known that grain size strongly influences the surface roughness of polycrystalline ZnO thin films. However, although thin films annealed with lower energy densities had finer average grain size, they had rugged surfaces. As a result, their RMS roughness values were greater than that of the ELA 150 thin film. Moreover, the RMS roughness value of the TA thin film (7.60 nm) was greater than that of the ELA 150 thin film (5.30 nm) because the surface of the TA thin film had fiber-like streaks and wrinkles [22].

Plane-view SEM micrographs of ZnO thin films fabricated by thermal annealing and excimer laser annealing are shown in Fig. 5. Fig. 5(a) is a SEM image of the TA thin film; it displays nano-size particles and some nano-voids, which can degrade a film's electrical properties. The SEM image of the ELA 150 thin film (Fig. 5(b)) shows its densified microstructure, consisting of equiaxed grains in the film. Nagase et al. reported that the excimer laser annealing process was a simpler way to produce closed-packed crystals than the conventional thermal annealing process [17]. Tsang et al. proposed that carrier mobility rose and electrical resistivity fell in laser irradiated ZnO-based films because grain-boundary densities and crystal lattice defects in the films were reduced by laser irradiation treatment [18]. Comparing Fig. 5(a) and (b), it is well demonstrated that annealing the ZnO sol–gel films by excimer laser irradiation produces high-quality ZnO thin films.

However, a few dark lines along the grain boundaries, indicating microcracks, can also be observed in Fig. 5(b). The intergranular microcracks formed due to local non-uniform tensile stress induced by the rapid cooling rate after irradiation with excimer laser energy. It is suggested that combining a direct printing technique of material solutions with the excimer laser annealing process may reduce the magnitude of non-uniform tensile stress, allowing the preparation of crack-free ZnO thin films.

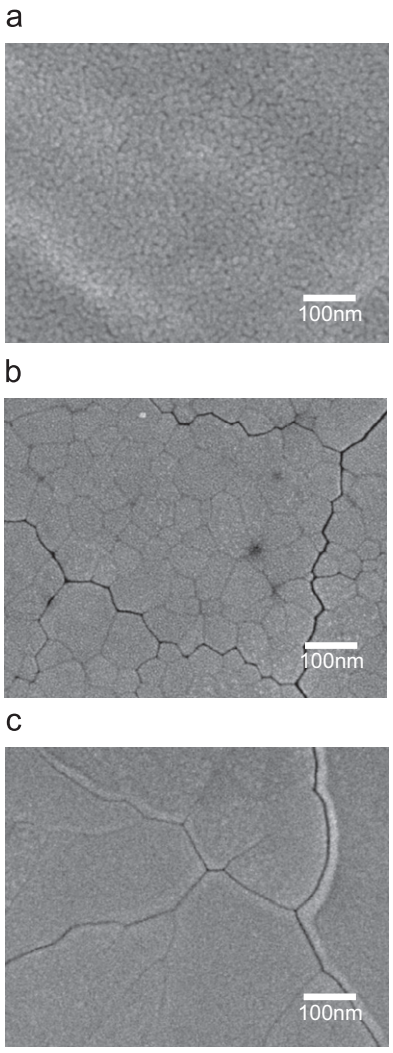


Fig. 5. Plane-view SEM micrographs of (a) thermally annealed (TA) thin film and dried sol–gel films by annealed excimer laser at energy densities of (b) 150 mJ/cm$^2$ (ELA 150), and (c) 175 mJ/cm$^2$ (ELA 175).

A micrograph of the ELA 175 thin film (Fig. 5(c)) shows that the film's surface had clear grain boundaries and large abnormal grains, and grain size was greater than that of the ELA 150 thin film. XRD examination showed that a strong (103) peak appeared when the laser energy density achieved 175 mJ/cm$^2$ (spectrum of (vi) in Fig. 2), indicating that the samples underwent abnormal grain growth. That SEM image provides direct evidence that annealing dried ZnO sol–gel films with the highest energy density used in this study will induce abnormal grain growth.

The optical transmittance spectra of TA and ELA ZnO thin films, with wavelengths from 200 to 850 nm, are shown in Fig. 6. All transmittance spectra exhibited sharp absorption in the wavelength region between 350 and 390 nm. Each film's absorption edge was evaluated from a plot of $dT/d\lambda$ vs. wavelength ($\lambda$), where $T$ is the transmittance of the film. The wavelength of the absorption edge of the TA thin film was 378 nm, and those of the ELA 125, 150, and 175 thin films were 366, 361, and 361 nm. The absorption wavelength value

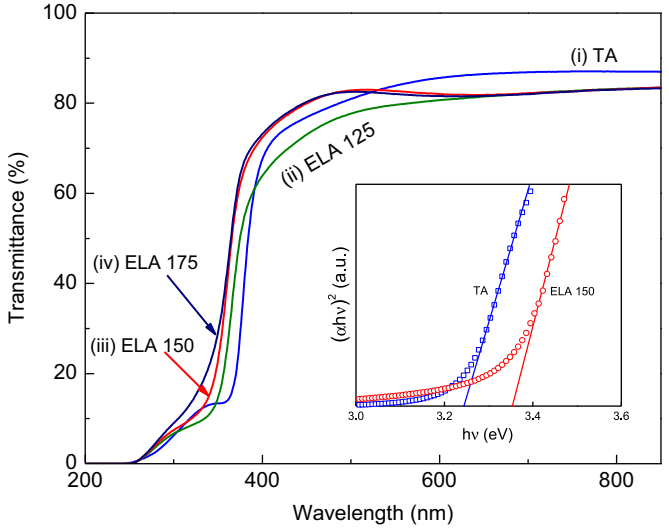


Fig. 6. Optical transmittance spectra of thermally and excimer laser annealed ZnO thin films. The inset is the plot of $(\alpha hv)^2$ vs. photon energy of the corresponding samples.

shifted slightly to shorter wavelengths as the laser energy density increased from 125 to 150 mJ/cm$^2$. Table 1 summarizes the transmittance range in the wavelengths between 400 and 800 nm for TA and ELA 150 thin films. At a wavelength of 550 nm, two samples exhibited similar optical transparency ($T > 82.5\%$). However, the ELA 150 thin film had lower transparency than the TA thin film, possibly due to light scattering arising from the grain boundaries and microcracks.

The absorption coefficient ($\alpha$) of transparent thin film can be calculated by the formula $\alpha = (1/t)\ln(1/T)$, where $t$ is the film thickness. The mean thickness of TA and ELA 150 thin films, evaluated from the cross-sectional SEM micrographs, were 140 and 85 nm, respectively (data not shown). The absorption coefficient of direct band gap materials can be written as the following formula for estimating the optical band gap [23],

$$(\alpha hv) = B(hv - E_g)^{1/2}, \quad (1)$$

where $hv$ is the photon energy, $B$ is a constant, and $E_g$ is the optical band gap. The optical band gap was determined by extrapolating the straight section of the plot of $(\alpha hv)^2$ vs. photon energy (shown in the inset of Fig. 6). The determined $E_g$ values of TA and ELA 150 thin films were 3.24 and 3.38 eV, respectively. The band gap of the ELA 150 ZnO thin film is close to that a ZnO crystal (3.4 eV) [21], representing that the film has good quality, namely low grain-boundary density and high densification. The narrow band gap of TA ZnO thin films as compared to that of sputtered ZnO thin films (3.3 eV) [24] may be attributed to the greater number of grain boundaries and existence of nano-voids, which increase band tailing in the band gap [23].

Excimer laser annealing induces changes in crystallization, microstructure, surface morphology, and optical transmittance in sol–gel derived ZnO thin films. Dried

ZnO sol–gel films irradiated with a laser energy density of 150 mJ/cm$^2$ exhibited good crystallization, high densification, and a flat surface. Control of this process with optimum processing parameters could be integrated with direct printing techniques for realizing the manufacture of low-cost, high-performance transparent electronics.

## 4. Conclusions

Crystallized ZnO thin films have been prepared by excimer laser annealing of ZnO sol–gel films on alkali-free glass substrates at low temperature of 300 °C. All excimer laser annealed ZnO thin films possessed the hexagonal wurtzite structure and exhibited a strong growth orientation along the (101) plane. We have demonstrated that KrF excimer laser annealing can significantly improve the crystallinity level, densification, and surface flatness of sol–gel derived ZnO thin films. However, the highest laser irradiation energy density in this study (175 mJ/cm$^2$) induced abnormal grain growth in the films. In the present study, dried ZnO sol–gel films annealed with the optimum energy density of 150 mJ/cm$^2$ had a dense and cellular-type microstructure, obtained a minimum RMS roughness of 5.30 nm, exhibited a transmittance of over 82.5% for a wavelength of 550 nm, and had an optical band gap of 3.38 eV. The hybrid sol–gel spin coating/excimer laser annealing process could be applied to the fabrication of high-performance optical/electrical devices.

## Acknowledgments

This study received financial support from the Taiwan TFT-LCD Association (TTLA) under Contract no. A643TT1000-S11. The authors gratefully acknowledge Prof. I-Nan Lin in Tamkang University for help excimer laser annealing process and the Precision Instrument Support Center of Feng Chia University in providing the measurement facilities.

## References

[1] S.Y. Park, B.J. Kim, K. Kim, M.S. Kang, K.H. Lim, T.I. Lee, J.M. Myoung, H.K. Baik, J.H. Cho, Y.S. Kim, Low-temperature, solution-processed and alkali metal doped ZnO for high performance thin-film transistors, Advanced Materials 24 (2012) 834–838.

[2] H. Bong, W.H. Lee, D.Y. Lee, B.J. Kim, J.H. Cho, K. Cho, High mobility low-temperature ZnO transistors with low-voltage operation, Applied Physics Letters 96 (2010) 192115.

[3] S.S. Shinde, K.Y. Rajpure, Fast response ultraviolet Ga-doped ZnO based photoconductive detector, Materials Research Bulletin 46 (2011) 1734–1737.

[4] K. Kinoshita, T. Okutani, H. Tanaka, T. Hinoki, H. Agura, K. Yazawa, K. Ohmi, S. Kishida, Flexible and transparent ReRAM with GZO memory layer and GZO-electrodes on large PEN sheet, Solid-State Electronics 58 (2011) 48–53.

[5] L.M. Wong, S.Y. Chiam, J.Q. Huang, S.J. Wang, W.K. Chim, J.S. Pan, Examining the transparency of gallium-doped zinc oxide for photovoltaic applications, Solar Energy Materials and Solar Cells 95 (2011) 2400–2406.

[6] J. Eriksson, V. Khranovskyy, F. Söderlind, P.O. Käll, R. Yakimova, A.L. Spetz, ZnO nanoparticles or ZnO films: a comparison of the gas sensing capabilities, Sensors and Actuators B: Chemical 137 (2009) 94–102.

[7] Y.Q. Fu, J.K. Luo, X.Y. Du, A.J. Flewitt, Y. Li, G.H. Markx, A.J. Walton, W.I. Milne, Recent developments on ZnO films for acoustic wave based bio-sensing and microfluidic applications: a review, Sensors and Actuators B: Chemical 143 (2010) 606–619.

[8] N. Yamamoto, H. Makino, S. Osone, A. Ujihara, T. Ito, H. Hokari, T. Maruyama, T. Yamamoto, Development of Ga-doped ZnO transparent electrodes for liquid crystal display panels, Thin Solid Films 520 (2012) 4131–4138.

[9] K. Song, J. Noh, T. Jun, Y. Jung, H.Y. Kang, J. Moon, Fully flexible solution-deposited ZnO thin-film transistors, Advanced Materials 22 (2010) 4308–4312.

[10] M.G. Kim, M.G. Kanatzidis, A. Facchetti, T.J. Marks, Low-temperature fabrication of high-performance metal oxide thin-film electronics via combustion processing, Nature Materials 10 (2011) 382–388.

[11] Y.H. Yang, S.S. Yang, K.S. Chou, Performance improvements of IGZO and ZnO thin-film transistors by laser-irradiation treatment, Journal of the Society for Information Display 19 (2011) 247–252.

[12] T. Nagase, T. Ooie, J. Sakakibara, A novel approach to prepare zinc oxide films: excimer laser irradiation of sol–gel derived precursor films, Thin Solid Films 357 (1999) 151–158.

[13] D. Bao, H. Gu, A. Kuang, Sol–gel derived *c*-axis oriented ZnO thin films, Thin Solid Films 312 (1998) 37–39.

[14] Y. Zhao, Y. Jiang, Effect of KrF excimer laser irradiation on the properties of ZnO thin films, Journal of Applied Physics 103 (2008) 114903.

[15] M. Nakata, K. Takechi, K. Azuma, E. Tokumitsu, H. Yamaguchi, S. Kaneko, Improvement of $InGaZnO_4$ thin film transistors characteristics utilizing excimer laser annealing, Applied Physics Express 2 (2009) 021102.

[16] J.J Kim, J.Y. Bak, J.H. Lee, H.S. Kim, N.W. Jang, Y. Yun, W.J. Lee, Characteristics of laser-annealed ZnO thin film transistors, Thin Solid Films 518 (2010) 3022–3025.

[17] T. Nagase, T. Ooie, Y. Makita, M. Nakatsuka, K. Shinozaki, N. Mizutani, A novel method for the preparation of green photoluminescent undoped zinc oxide film involving excimer laser irradiation of a sol–gel derived precursor, Japanese Journal of Applied Physics 39 (2000) L713–L715.

[18] W.M. Tsang, F.L. Wong, M.K. Fung, J.C. Chang, C.S. Lee, S.T. Lee, Transparent conducting aluminum-doped zinc oxide thin film prepared by sol–gel process followed by laser irradiation treatment, Thin Solid Films 517 (2008) 891–895.

[19] K. Kim, S. Kim, S.Y. Lee, Effect of excimer laser annealing on the properties of ZnO thin film prepared by sol–gel method, Current Applied Physics 12 (2012) 585–588.

[20] H.C. Cheng, C.F. Chen, C.Y. Tsay, J.P. Leu, High oriented ZnO films by sol–gel and chemical bath deposition combination method, Journal of Alloys and Compounds 475 (2009) L46–L49.

[21] D.P. Norton, Y.W. Heo, M.P. Ivill, K. Ip, S.J. Pearton, M.F. Chisholm, T. Steiner, ZnO: growth, doping and processing, Materials Today 7 (2004) 34–40.

[22] C.Y. Tsay, M.C. Wang, S.C. Chiang, Characterization of $Zn_{1-x}Mg_xO$ films prepared by the sol–gel process and their application for thin-film transistors, Journal of Electronic Materials 38 (2009) 1962–1968.

[23] Y. Caglar, M. Caglar, S. Ilican, Microstructural, optical and electrical studies on sol–gel derived ZnO and ZnO:Al films, Current Applied Physics 12 (2012) 963–968.

[24] K.H. Kim, K.C. Park, D.Y. Ma, Structural, electrical and optical properties of aluminum doped zinc oxide films prepared by radio frequency magnetron sputtering, Journal of Applied Physics 81 (1997) 7764–7772.